AMERICAN SOCIETY FOR MICROBIOLOGY | Antimicrobial Agents and Chemotherapy®

ANTIVIRAL AGENTS

# Nucleoside Analogs with Selective Antiviral Activity against Dengue Fever and Japanese Encephalitis Viruses

**Keivan Zandi,[a,b] Leda Bassit,[a] Franck Amblard,[a] Bryan D. Cox,[a] Pouya Hassandarvish,[b] Ehsan Moghaddam,[b] Andrew Yueh,[c] Gisele Olinto Libanio Rodrigues,[d] Ingredy Passos,[d] Vivian V. Costa,[d] Sazaly AbuBakar,[b] Longhu Zhou,[a] James Kohler,[a] Mauro M. Teixeira,[a,d] Raymond F. Schinazi[a]**

[a]Center for AIDS Research, Laboratory of Biochemical Pharmacology, Department of Pediatrics, Emory University School of Medicine, Atlanta, Georgia, USA
[b]Tropical Infectious Disease Research and Education Center, Department of Medical Microbiology, Faculty of Medicine, University of Malaya, Kuala Lumpur, Malaysia
[c]Institute of Biotechnology and Pharmaceutical Research, National Health Research Institutes, Taiwan, Republic of China
[d]Center for Research and Drug Development, Instituto de Ciencias Biológicas, Universidade Federal de Minas Gerais, Belo Horizonte, Brazil

**ABSTRACT** Dengue virus (DENV) and Japanese encephalitis virus (JEV) are important arthropod-borne viruses from the *Flaviviridae* family. DENV is a global public health problem with significant social and economic impacts, especially in tropical and subtropical areas. JEV is a neurotropic arbovirus endemic to east and southeast Asia. There are no U.S. FDA-approved antiviral drugs available to treat or to prevent DENV and JEV infections, leaving nearly one-third of the world's population at risk for infection. Therefore, it is crucial to discover potent antiviral agents against these viruses. Nucleoside analogs, as a class, are widely used for the treatment of viral infections. In this study, we discovered nucleoside analogs that possess potent and selective anti-JEV and anti-DENV activities across all serotypes in cell-based assay systems. Both viruses were susceptible to sugar-substituted 2′-*C*-methyl analogs with either cytosine or 7-deaza-7-fluoro-adenine nucleobases. Mouse studies confirmed the anti-DENV activity of these nucleoside analogs. Molecular models were assembled for DENV serotype 2 (DENV-2) and JEV RNA-dependent RNA polymerase replication complexes bound to nucleotide inhibitors. These models show similarities between JEV and DENV-2, which recognize the same nucleotide inhibitors. Collectively, our findings provide promising compounds and a structural rationale for the development of direct-acting antiviral agents with dual activity against JEV and DENV infections.

**KEYWORDS** Dengue virus, Japanese encephalitis virus, antiviral agents, nucleoside analogs

Dengue virus (DENV) and Japanese encephalitis virus (JEV) are members of the genus *Flavivirus*, belonging to the family *Flaviviridae*. Many flaviviruses are arthropod borne and cause severe infections in humans and vertebrate animals. DENV has four serotypes (DENV-1 to DENV-4), which collectively pose a health threat to 2.5 billion people worldwide, with 50 million to 100 million human infections and 500,000 cases of dengue hemorrhagic fever (DHF) and dengue shock syndrome (DSS) annually (1–3). JEV is one of the most important neurotropic flaviviruses that causes encephalitis in humans. Symptoms range from mild febrile illness to mortal illness, especially in children, with about 67,900 cases each year (4). JEV is endemic in eastern and southern Asia (including China, Indonesia, Nepal, Thailand, Saipan Island, Pakistan, and the Torres Strait) and Australia, with fatality rates of 20% to 30% and life-long neurological impairments and sequelae among one-half of the survivors (5–8). Despite a licensed vaccine to prevent JEV infection, infections occur annually due to a lack of complete coverage and access (9). A tetravalent DENV vaccine also exists but remains partially

**Citation** Zandi K, Bassit L, Amblard F, Cox BD, Hassandarvish P, Moghaddam E, Yueh A, Libanio Rodrigues GO, Passos I, Costa VV, AbuBakar S, Zhou L, Kohler J, Teixeira MM, Schinazi RF. 2019. Nucleoside analogs with selective antiviral activity against dengue fever and Japanese encephalitis viruses. Antimicrob Agents Chemother 63:e00397-19. https://doi.org/10.1128/AAC.00397-19.



Address correspondence to Raymond F. Schinazi, rschina@emory.edu.

**Received** 21 February 2019
**Returned for modification** 5 March 2019
**Accepted** 3 May 2019
**Accepted manuscript posted online** 6 May 2019
**Published** 24 June 2019

effective (10) and recently was withdrawn by the manufacturer (11). Importantly, there are no approved and efficient antiviral agents for the prevention and treatment of these severe pathogens. Therefore, effective antiviral modalities that reduce morbidity and mortality rates for these infections are essential.

Nucleoside analogs represent a well-established class of antiviral agents that inhibit viral replication. Notable drugs in this class are emtricitabine and tenofovir disoproxil fumarate for HIV-1 infections and sofosbuvir as the curative agent for hepatitis C virus (HCV) infections (12, 13). These drugs are delivered as nucleoside or nucleotide prodrugs, which are then processed by host kinases to the active nucleoside triphosphate (NTP) analog. The NTP analog is then misincorporated by viral polymerase into the growing viral genome, halting replication. Flaviviruses encode a conserved RNA-dependent RNA polymerase (RdRp) enzyme responsible for replicating the positive-sense RNA genome (14, 15).

To address the paucity of effective nucleoside inhibitors, a small library of 14 nucleoside analogs was evaluated for the ability to inhibit DENV and JEV replication in cell culture. Among the analogs, four compounds inhibited replication of JEV and all DENV serotypes and demonstrated efficacy in a mouse model of DENV-2 infection. Two of the compounds demonstrated dual selective *in vitro* antiviral activity against JEV and DENV.

## RESULTS

**Cytotoxicity study.** Nucleosides and nucleotide prodrugs (Fig. 1) were first subjected to a cytotoxicity assay using MTS [3-(4,5-dimethylthiazol-2-yl)-5-(3-carboxymethoxyphenyl)-2-(4-sulfophenyl)-2*H*-tetrazolium] in BHK-21 and Vero cells (corresponding to cell lines used for antiviral activity). All compounds exhibited minimal toxicity up to 100 $\mu$M in both Vero and BHK cell lines. The maximum nontoxic concentration (MNTC), at which 90% of the cells were viable, was $>$50 $\mu$M for all compounds (Table 1). Subsequent antiviral assays were conducted at concentrations lower than the MNTC.

**Nucleoside inhibitors of JEV.** A replicon assay using a rapid luciferase-based readout was used to evaluate potential antiviral activity. Fourteen compounds were evaluated for potential antiviral activity using a JEV replicon cell line. Among them, compounds 3, 5, and 10 exhibited significant inhibitory effects in JEV replicon cells (Fig. 2A), with compound 10 showing the strongest anti-JEV activity (50% effective concentration [$EC_{50}$] of 2.3 $\mu$M). The remaining compounds did not show efficient inhibition of JEV at concentrations up to 50 $\mu$M. The three active compounds (compounds 3, 5, and 10) identified during our initial JEV replicon evaluation were then tested against a replication-competent virus. As expected, each of these compounds exhibited potent anti-JEV activity in a focus-forming unit reduction assay (FFURA) (Fig. 3A). Compounds 3, 5, and 10 were tested in a concentration-dependent manner, using a virus yield reduction assay with a quantitative reverse transcription (qRT)-PCR readout (Fig. 3B), and showed potent inhibitory activity against *in vitro* replication of JEV in Vero cells (90% effective concentration [$EC_{90}$] values of 4.5, 3.9, and 4.7 $\mu$M, respectively) (Table 2).

**Molecular model of JEV RdRp replication complex.** To better understand how nucleotide antiviral agents are recognized by the viral polymerase, a molecular model of the JEV RdRp replication complex bound to the triphosphate form of compound 10 in the active site was constructed (Fig. 4). Several crystal structures of the JEV RdRp exist, providing molecular insight into the overall structure of the protein. However, these structures lack the RNA template/primer and catalytic active site metals. The recent structures of the HCV RdRp with RNA template/primer and incoming nucleotide serve as valuable templates to build models of the tertiary JEV replication complex. JEV residues in contact with the nucleic RNA template/primer were modeled using the HCV structural template (16), and residues not in contact with the nucleic components were kept in the same conformation as in the JEV crystal structure (17). The structure was further refined by multiple rounds of molecular minimization using Prime. The 7-deaza-

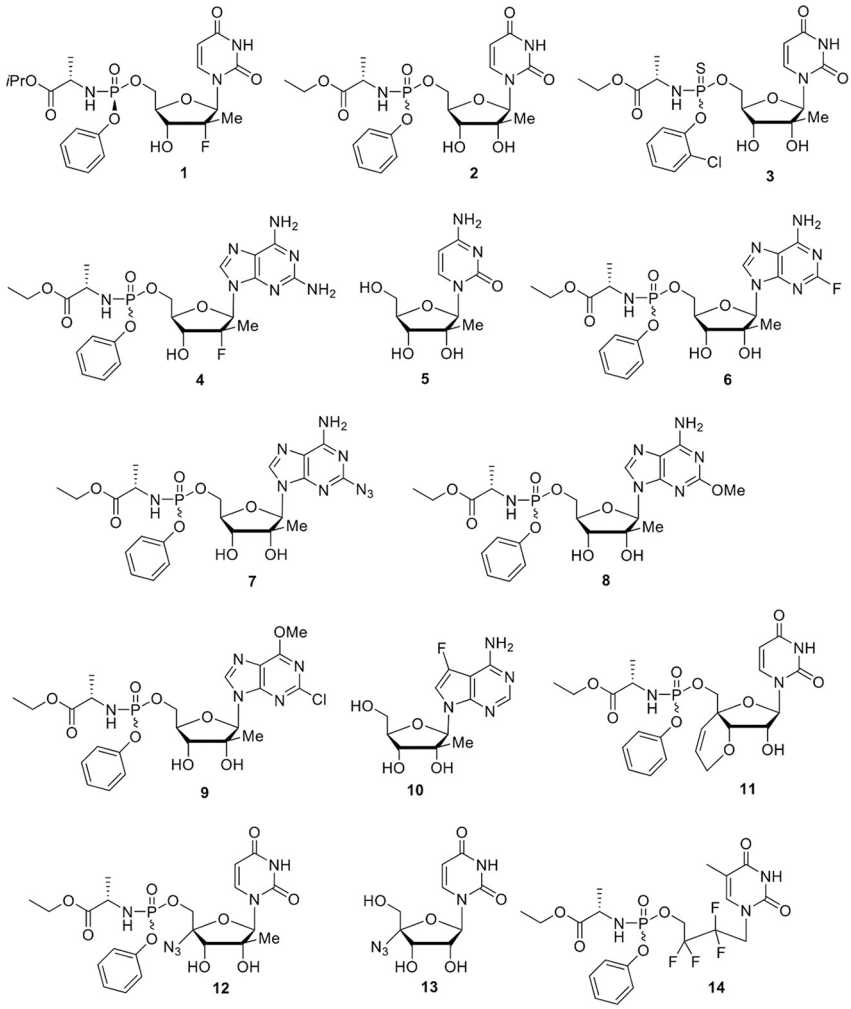

**FIG 1** Chemical structures of nucleoside analogs 1 to 14.

7-fluoro-adenine base forms canonical base pair bonds with the template uridine and planar stacking interactions with Arg474. The 2′-OH group contributes to a hydrogen bonding network with Ser604 and Asn613. The 2′-*C*-methyl group is positioned in a hydrophobic pocket formed by the $\beta$-carbon of Ser604 and the $\beta$- and $\gamma$-carbons of

**TABLE 1** Cytotoxicity of nucleoside analogs in Vero and BHK-21 cells using an MTS assay

| Compound | Vero cells | | BHK-21 cells | |
|---|---|---|---|---|
| | $CC_{50}$ ($\mu$M) | MNTC ($\mu$M) | $CC_{50}$ ($\mu$M) | MNTC ($\mu$M) |
| 1 | >200 | 52 | >200 | 50 |
| 2 | >200 | 50 | >200 | >50 |
| 3 | >200 | >100 | >200 | >100 |
| 4 | >200 | 50 | >200 | >50 |
| 5 | >200 | >50 | >200 | >50 |
| 6 | >200 | >50 | >200 | >50 |
| 7 | >200 | >50 | >200 | >50 |
| 8 | >200 | >100 | >200 | >100 |
| 9 | >200 | >100 | >200 | >100 |
| 10 | >200 | >50 | >200 | >50 |
| 11 | >200 | 50 | >200 | 50 |
| 12 | >200 | >50 | >200 | 51 |
| 13 | >200 | >50 | >200 | >50 |
| 14 | >100 | >100 | >200 | >100 |
| Cycloheximide | 0.2 | 0.09 | 0.16 | 0.1 |

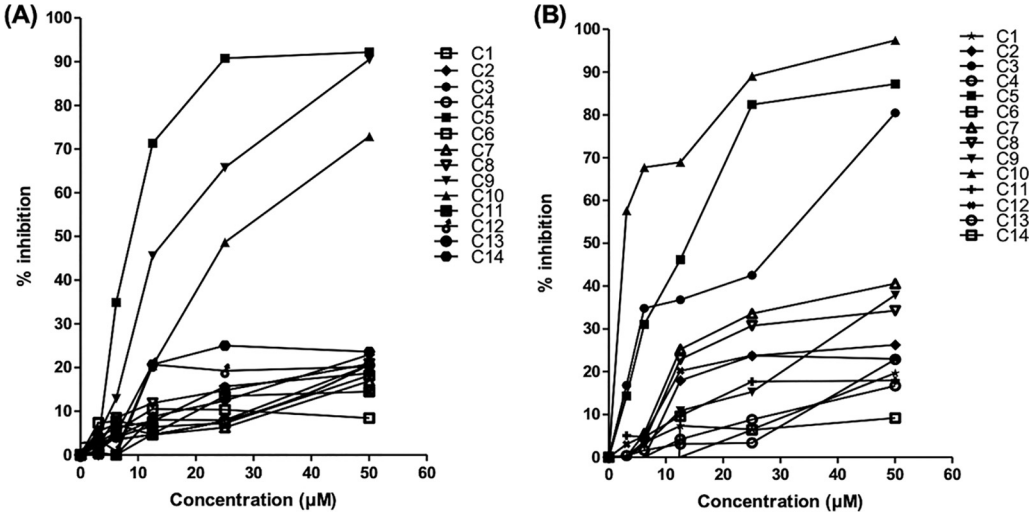


**FIG 2** Primary antiviral evaluation of nucleoside analogs. (A) DENV replicon cell line. (B) JEV replicon cell line. All 14 nucleoside/nucleotide prodrug compounds (C1 to C14) were evaluated in the DENV and JEV replicon systems at five concentrations. Percent inhibition, relative to untreated controls, is plotted versus concentration for each compound. Of the 14 compounds tested, compounds 3, 5, and 10 exhibited significant inhibitory activity against JEV and compounds 5, 9, and 10 showed significant inhibitory activity against DENV-2 in a replicon cell line.

Arg474. The triphosphate group forms electrostatic interactions with Arg474, Lys694, and two active site $Mn^{2+}$ ions.

**Nucleoside inhibitors of DENV.** The same 14 nucleoside analogs were assayed against DENV using a BHK-21 cell line harboring the DENV-2 replicon system. Compounds 5, 9, and 10 exhibited the most potent inhibitory activities in this assay (Fig. 2B). Among them, compound 10 showed the most potent ($EC_{50}$ of 0.8 $\mu$M) and

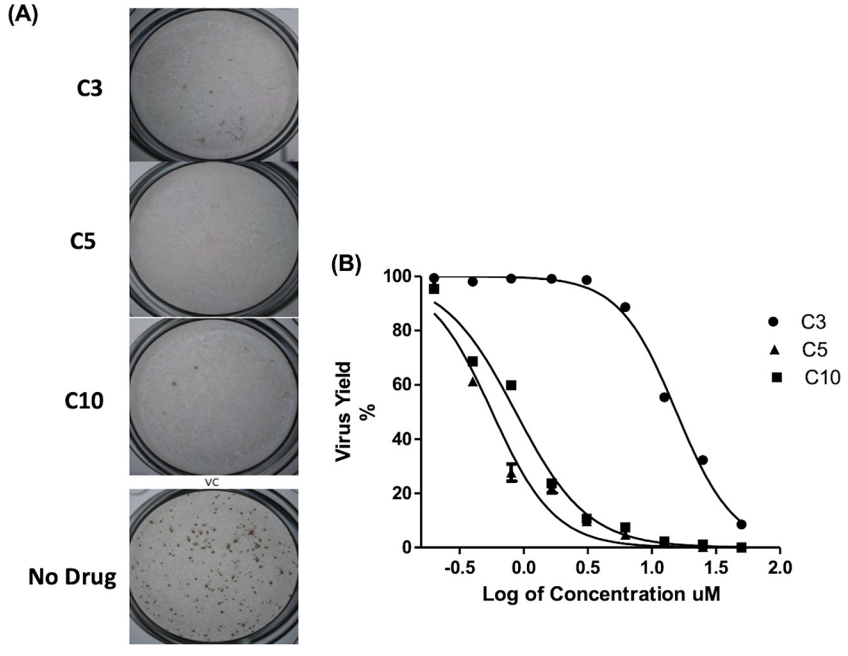


**FIG 3** Inhibition of JEV replication by nucleoside/nucleotide prodrug analogs. (A) FFURA. Compounds 3, 5, and 10 showed significant inhibitory effects against JEV focus presentation, compared to untreated and infected controls, at 25 $\mu$M. (B) Virus yield reduction assay data. Compounds 3, 5, and 10 inhibited the Nakayama strain of JEV in Vero cells in a dose-dependent manner, using qRT-PCR for the virus yield assay. Results are presented as the means ± SDs from triplicate assays from three independent experiments. The solid lines represent the fits of the data points to obtain $EC_{50}$ and $EC_{90}$.

**TABLE 2** $EC_{50}$ and $EC_{90}$ values of nucleoside analogs for JEV in Vero cells by qRT-PCR[a]

| Compound | $EC_{50}$ ($\mu$M) | $EC_{90}$ ($\mu$M) |
|---|---|---|
| 3 | 15.7 ± 0.26 | 48.8 ± 0.7 |
| 5 | 0.66 ± 0.12 | 2.27 ± 0.41 |
| 10 | 0.85 ± 0.17 | 3.5 ± 0.53 |

[a]All values are means ± SDs.

specific activity against the DENV-2 replicon, followed by compounds 5 and 9 (Fig. 2B).

Active agents identified in the initial replicon evaluation were then tested against replication-competent DENV from all four serotypes using the FFURA. Compounds 5, 9, and 10 inhibited the formation of DENV foci by all serotypes at 50 $\mu$M, thereby confirming antiviral activity (Fig. 5A). To quantitate potency, these three agents were evaluated in the virus yield reduction assay at various concentrations, with qRT-PCR readout (Fig. 5B). The three compounds reduced viral production by all serotypes in a concentration-dependent manner. Compound 10 was the most effective, demonstrating potent activity against DENV-2 ($EC_{50}$ of 0.4 $\mu$M) (Table 3). Compound 5 also showed inhibitory activity against all DENV serotypes, with the lowest $EC_{50}$ value against DENV-3 ($EC_{50}$ of 2.4 $\mu$M), followed by DENV-4, DENV-2, and DENV-1 ($EC_{50}$ values of 2.6, 2.8, and 2.9 $\mu$M, respectively). Compound 9 was the least active agent of the three, with $EC_{50}$ values ranging from 9.9 $\mu$M against DENV-3 to 12.9 $\mu$M against DENV-4, but without significant toxicity in Vero cells (50% cytotoxic concentration [$CC_{50}$] of >200 $\mu$M).

**Molecular model of DENV RdRp replication complex.** Like those for JEV, many structures for DENV-2 and DENV-3 RdRp are available but lack information regarding the replication complex, RNA template/primer, and active site. A model of the DENV RdRp replication complex with the triphosphate form of compound 10 in the active site was generated using an approach similar to that described for JEV. DENV-2 (PDB accession no. 5K5M) was utilized because this structure resolves residues near the proposed active site (see Materials and Methods) (18). Loops near the RNA template/primer and active sites were modeled using the HCV replication complex, and the remaining protein was positioned in accordance with the DENV-2 structure. This model indicated that the 7-deaza-7-fluoro adenine nucleobase forms canonical hydro-

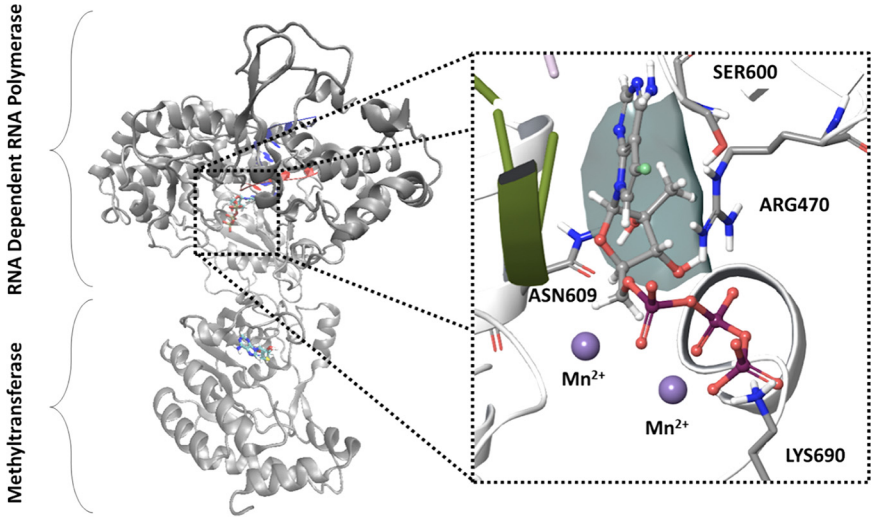


**FIG 4** Molecular model of the JEV replication complex with compound 10 triphosphate in the active site. The full-length JEV NS5 was used as a structural template for both RdRp and methyltransferase subunits. Residues near the RNA template/primer and the active site were modeled using the HCV replication complex. Inset, key protein-ligand interactions within the active site, showing the 2′-*C*-methyl pocket formed by Arg470 and Ser600 (surface).

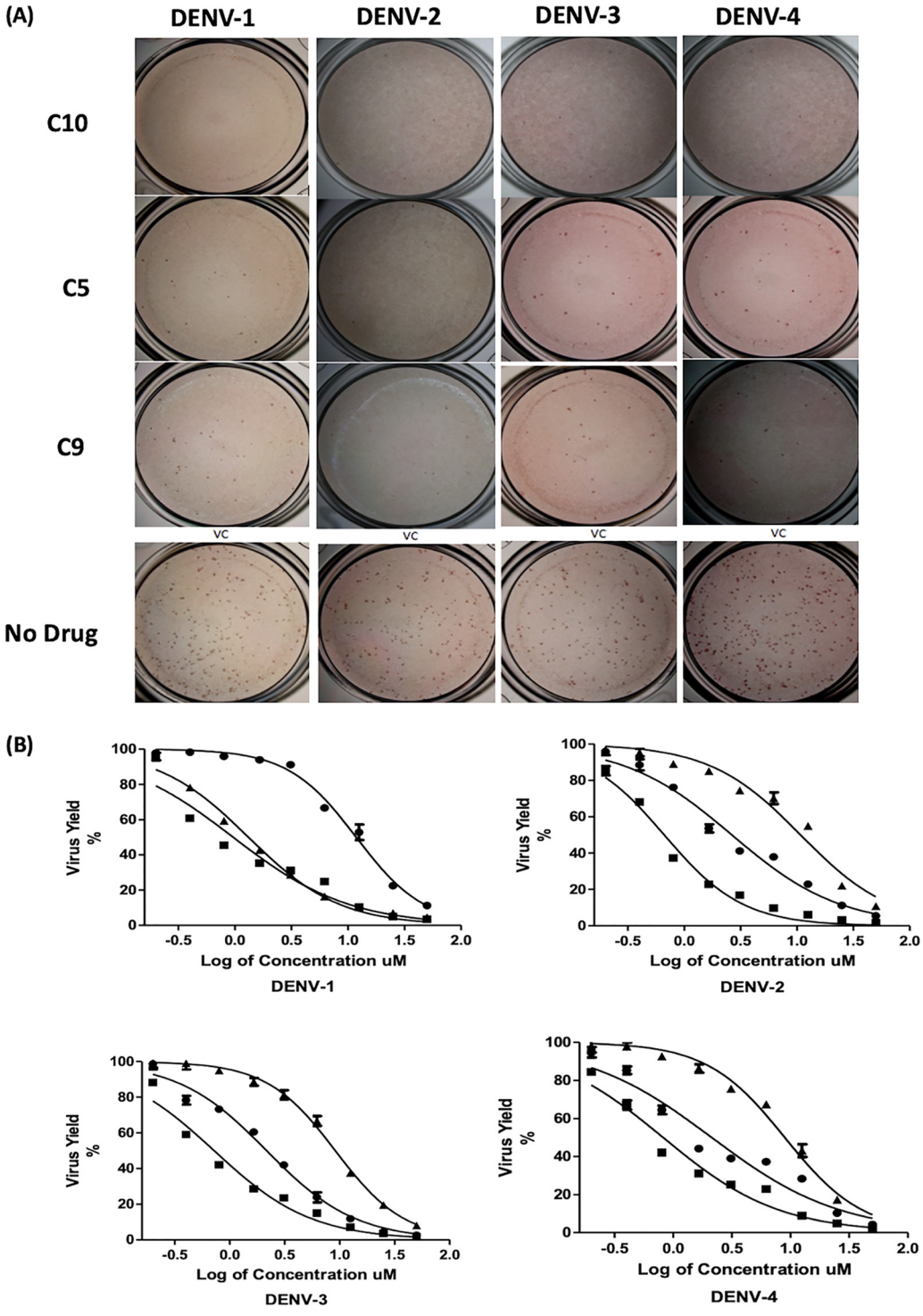


**FIG 5** Inhibition of DENV replication by nucleoside/nucleotide prodrug analogs. (A) FFURA. FFURA images for compounds 5, 9, and 10 at 25 $\mu$M against each DENV serotype, compared to untreated controls, are shown. (B) Virus yield assay. Effects of compounds 5 (circles), 9 (triangles), and 10 (squares) on DENV yields in dose-response assays for each serotype were evaluated using qRT-PCR. Results are presented as the means ± SDs from triplicate assays from three independent experiments. The fits of the data points to obtain $EC_{50}$ and $EC_{90}$ values are provided (solid lines).

gen bonds with the template and stacks with Arg207 (Fig. 6). The 7-fluoro moiety interacts with Arg472, particularly with NεH (3.10 Å) and the imine $=NH_2^+$ (3.58 Å). The 2′-*C*-methyl group occupies a pocket formed between Arg472 and Ser600. The triphosphate group is held in place by electrostatic interactions between Lys469, Arg472, Lys689, and two $Mn^{2+}$ ions.

**TABLE 3** Inhibitory activity of nucleoside analogs on DENV serotypes 1 to 4 in Vero cells using a qRT-PCR assay[a]

| | DENV-1 | | DENV-2 | | DENV-3 | | DENV-4 | |
|---|---|---|---|---|---|---|---|---|
| Compound | $EC_{50}$ ($\mu$M) | $EC_{90}$ ($\mu$M) | $EC_{50}$ ($\mu$M) | $EC_{90}$ ($\mu$M) | $EC_{50}$ ($\mu$M) | $EC_{90}$ ($\mu$M) | $EC_{50}$ ($\mu$M) | $EC_{90}$ ($\mu$M) |
| 5 | 2.9 ± 0.31 | 22.8 ± 0.9 | 2.8 ± 0.2 | 32 ± 1.2 | 2.4 ± 0.4 | 18.3 ± 0.9 | 2.6 ± 0.61 | 30.1 ± 0.9 |
| 9 | 12.2 ± 0.42 | 56 ± 1.6 | 11.1 ± 0.4 | 84.9 ± 0.9 | 9.9 ± 0.25 | 75.7 ± 0.8 | 12.5 ± 0.9 | 66.8 ± 0.85 |
| 10 | 0.96 ± 0.2 | 13.6 ± 1.4 | 0.46 ± 0.08 | 2.7 ± 0.9 | 0.85 ± 007 | 4.9 ± 0.6 | 0.87 ± 0.08 | 5.8 ± 0.8 |

[a]Results are means ± SDs from replicates.

***In vivo* activity against DENV-2.** Based on the compelling *in vitro* antiviral activity of compound 10 against flaviviruses, it was further assessed for efficacy using an *in vivo* model of DENV-2 infection in A129 mice. $A129^{-/-}$ mice were chosen because they are immunodeficient, specifically lacking type I alpha interferon (IFN-$\alpha$) and IFN-$\beta$ receptors. Type I IFNs (IFN-$\alpha$ and IFN-$\beta$) play significant roles in preventing viral replication and protecting against arboviral infections, including DENV infections (19, 20). They are the gold standard models to evaluate virus replication and therapeutic drugs, due their elevated susceptibility to infection. Here, A129 male mice were infected with $1 \times 10^3$ PFU of a clinical isolate of DENV-2 (strain 05K3295), resulting in elevated viral loads in serum, spleen, liver, and brain, as observed in the vehicle-treated control group, consistent with previous reports (Fig. 7A to D) (19, 21–23). Treatment with compound 10 (10 mg/kg, intraperitoneally [i.p.], once a day) on day 0 potently prevented viral replication in all organs (Fig. 7, blue symbols). Treatment with compound 10 at day 2 postinfection reduced DENV-2 replication in serum, spleen, and liver but not in brain (Fig. 7, red symbols). These results demonstrate that compound 10 exerts strong antiviral activity *in vivo* against DENV.

Several markers were evaluated to determine the effects of compound 10 in mitigating DENV-associated disease. DENV-2 infection in A129 mice decreases platelet levels at peak infection (Fig. 8A). Treatment of infected mice with compound 10 at day 0 of infection prevented thrombocytopenia induced by DENV infection. When administered 2 days postinfection, compound 10 restored platelet levels but not to the degree of uninfected controls. Accordingly, untreated mice exhibited significantly decreased body weight (a sign of morbidity) on days 3 to 6 postinfection, when mice were moribund and euthanized (Fig. 8B). In contrast, mice treated with compound 10 on day 0 retained healthy body weight through the 6-day study period. When mice were treated 2 days postinfection, there was a delay in the body weight loss of approximately 1 day, relative to the vehicle-treated control group.

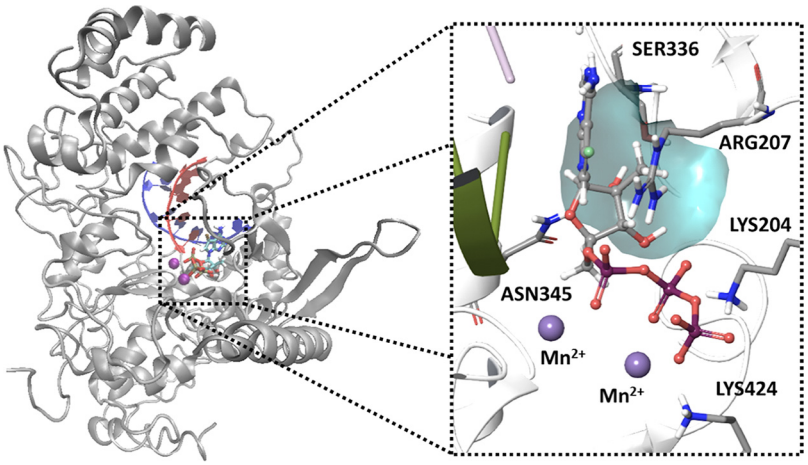


**FIG 6** Molecular model of the DENV-2 replication complex with compound 10 triphosphate in the active site. DENV-2 RdRp was used as a structural template, and residues near the RNA template/primer and the active site were modeled using the HCV replication complex. Inset, key protein-ligand interactions within the active site, showing the 2′-*C*-methyl pocket formed by Arg207 and Ser336 (blue surface).

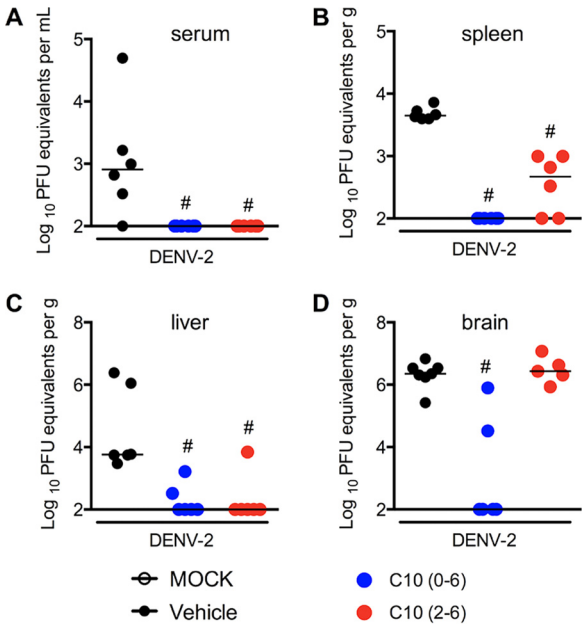


**FIG 7** Antiviral effects of compound 10 against DENV-2 *in vivo*. A129 mice (5 to 8 mice per group) were infected with DENV-2 ($1 \times 10^3$ PFU) on day 0, and viral loads were quantified with a plaque assay on day 6 postinfection. Compound 10 was administered daily (10 mg/kg), via the i.p. route, as a pretreatment (from day 0 to day 6) or therapeutically (from day 2 to day 6). Viral loads recovered from serum (A), spleen (B), liver (C), and brain (D) were determined. The median values for viral loads are represented as lines. #, $P < 0.05$, in comparison to the vehicle-treated infected group.

Leukocyte counts in blood were compared between mock-treated, vehicle-treated, and compound 10-treated mice (Fig. 8C). DENV-2 infection of A129 mice induced massive increases in total and differential leukocyte counts, including lymphocytes, neutrophils, and monocytes, by day 6 of infection. Similar to findings for platelets and weight loss, compound 10 treatment (initiated at either day 0 or day 2) resulted in statistically significant reductions in levels of circulating leukocytes, especially neutrophils.

Several markers of the inflammatory response to DENV infection were measured in control and compound 10-treated animals, namely, myeloperoxidase (MPO) activity in spleen and brain (indicative of neutrophil accumulation in tissues) and interleukin 6 (IL-6) and chemokine (C-C motif) ligand 5 (CCL5) serum levels (Fig. 8D and E). There were increases in MPO levels in spleen and brain and IL-6 and CCL5 levels in serum in DENV-infected mice, in comparison to control littermates. Administration of compound 10 as a pretreatment (day 0) or therapeutic administration (day 2 postinfection) greatly reduced neutrophil influx into the spleen and brain, to levels near those found in uninfected mice. These results parallel the observation that compound 10 treatment reduced levels of IL-6 and CCL5 in serum (Fig. 8D and E).

Lastly, hepatic damage induced by DENV-2 infection was assessed by histopathological analysis (Fig. 8H). In the vehicle-treated group, hepatic lesions were confirmed by the presence of inflammatory infiltrates concentrated in the perivascular area and spreading out into the liver parenchyma. The infiltrates were composed predominantly of polymorphonuclear and mononuclear cells, including neutrophils, macrophages, and multinucleated giant cells. Areas of hemorrhage and hepatocyte edema and degeneration were also evident in vehicle-treated mice. Compound 10 treatment of DENV-2-infected mice (either on day 0 or on day 2 postinfection) was associated with marked reductions in histopathological scores and decreases in hepatic damage (Fig. 8H).

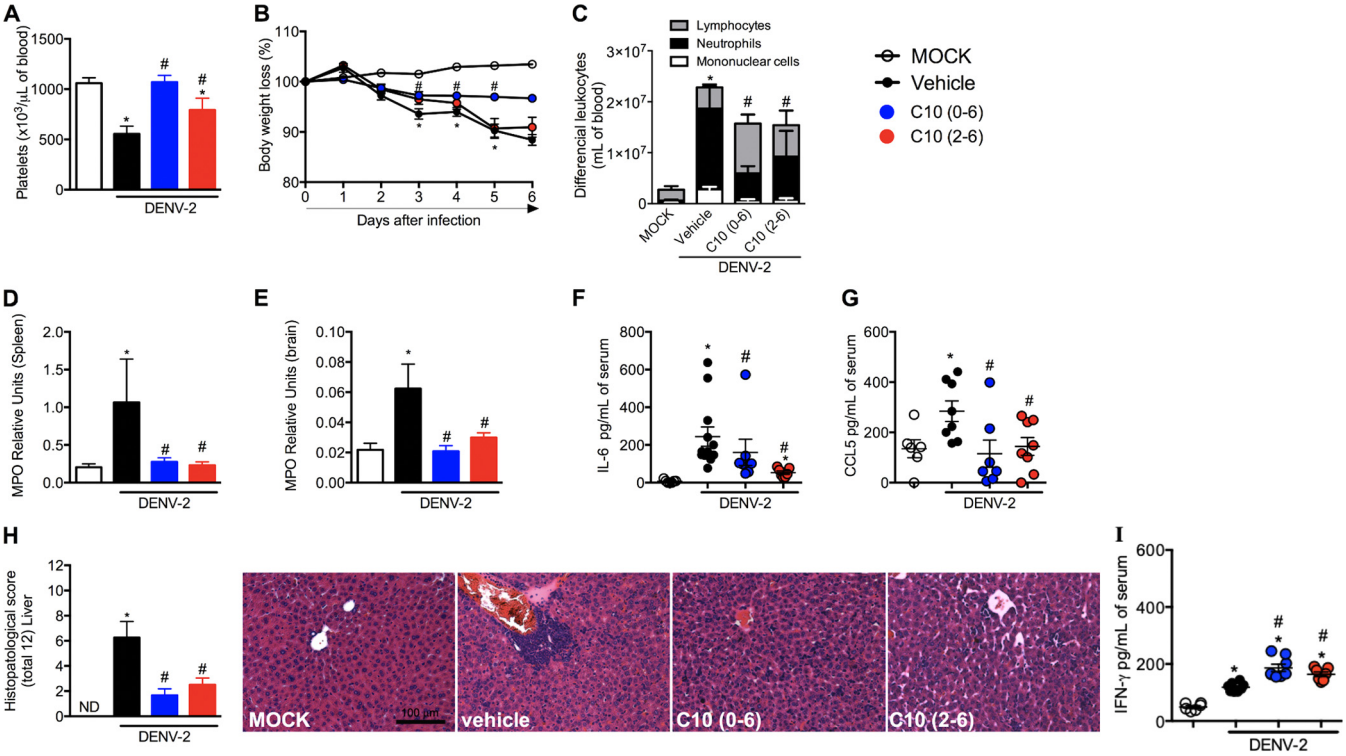


**FIG 8** Compound 10 prevention of disease caused by DENV-2 infection in infected mice. A129 mice (5 to 8 mice per group) were infected with DENV-2 ($1 \times 10^3$ PFU) on day 0. Disease and inflammatory parameters were measured on day 6 postinfection. Compound 10 was administered daily (10 mg/kg), via the i.p. route, as a pretreatment (starting on day 0) or therapeutically (starting on day 2 postinfection). (A) Numbers of platelets. (B) Changes in body weight, analyzed daily. Results are expressed as a percentage of initial weight loss after DENV-2 inoculation. (C) Total and differential cell counts in blood, represented as the numbers of different cell types (leukocytes, mononuclear cells, and neutrophils) normalized to the total cell counts. (D) Neutrophil influx into the spleen. (E) Neutrophil influx into the brain. (F) Concentrations of IL-6 in mouse serum. (G) Concentrations of CCL5 in mouse serum. (H) Semiquantitative analysis (histopathological score) and representative pictures for each group after hematoxylin and eosin staining of liver sections from control and DENV-2-infected mice, treated with compound 10 or not, 6 days after infection. ND, not determined. Original magnification, ×200. Scale bar, 100 $\mu$m. (I) Compound 10 induction of elevated IFN-$\gamma$ levels upon DENV-2 infection. Results are expressed as means ± SEMs and are representative of two experiments. *, $P < 0.05$, in comparison to the mock-treated group; #, $P < 0.05$, in comparison to the vehicle-treated infected group.

## DISCUSSION

Of the 14 nucleoside analogs evaluated, two compounds (compounds 5 and 10) potently and selectively inhibited JEV and all serotypes of DENV with minimal toxicity (summarized in Tables 1, 2, and 3). Compounds 5 and 10 are nucleoside analogs with a 2′-*C*-methyl sugar moiety, differing only in their respective bases. Compound 5 (2′-*C*-methyl-cytidine [2′-C-MeC]) has been reported previously as a potent inhibitor of certain flaviviruses (24). Compound 10 (7-deaza-7-fluoro-2′-*C*-methyl-adenosine [DFMA]) is chemically related to other 2′-*C*-methyl-adenosine derivatives known to inhibit flaviviruses such as HCV (25).

Since compounds 5 and 10 are also known to inhibit HCV RdRp, JEV, and all serotypes of DENV, DENV-2 models were compared to the HCV replication complex. All but three residues in direct contact with the incoming NTP are conserved among the three viruses, similar to observations reported with other flavivirus RdRp models (26). The active sites for binding to compound 10 are compared among DENV-2, JEV, and HCV in Fig. 9. Interestingly, despite possessing sequence identity near the 2′-OH group, 2′-deoxy-2′-fluoro analogs that inhibit HCV (compounds 1 and 4) showed no activity against DENV and JEV. However, *in vitro* anti-DENV activity of these two compounds in Huh-7 and human peripheral blood mononuclear cells was reported (27, 28). This is likely because prodrugs are not metabolized to the active drug in Vero cells, compared to cell systems with the right prodrug cleavage enzyme. Three residues differ between HCV and JEV/DENV-2 in the active site. There are also differences in the activities of compounds 3 and 9 against DENV and JEV, as the $EC_{50}$ for compound 3 against JEV was

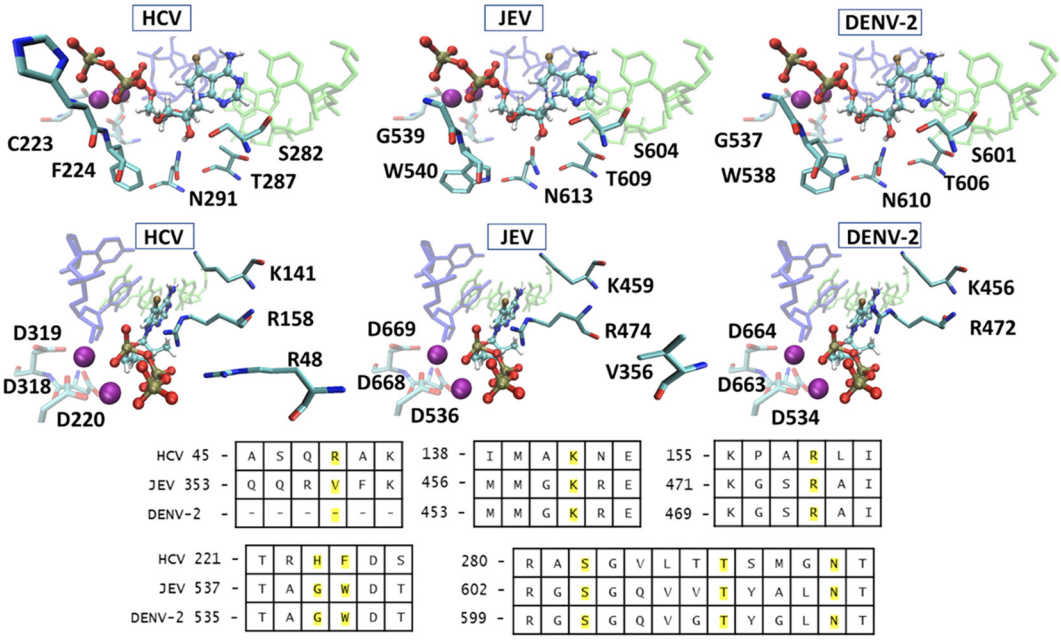


**FIG 9** Comparison of HCV, JEV, and DENV-2 active sites bound to 7-deaza-7-fluoro-2′-*C*-methyl-ATP. The RNA template and primer strands are shown in green and blue, respectively. The $Mn^{2+}$ ions are shown as purple spheres. The active site sequences from a stamp structural alignment for HCV, JEV, and DENV-2 are provided, and residues in direct contact with the incoming NTP are highlighted in yellow.

15.5 $\mu$M but the compound showed an inhibitory effect of just 20% against the DENV-2 replicon at 50 $\mu$M (Fig. 2B). In contrast, compound 9 exhibited an $EC_{50}$ of 12.5 $\mu$M against DENV-2 but showed only 38% inhibitory activity against the JEV replicon at 50 $\mu$M. The Arg48 residue in HCV is replaced by Lys in JEV/DENV-2 to retain interactions with the $\gamma$-phosphate group of the nucleotide. The His223 residue near the $\gamma$-phosphate group in HCV (wild-type Cys) is mutated to Gly in our models of JEV and DENV-2 replication. The Phe224 residue in HCV is positioned near the 4′-CH of the active site nucleotide, and this residue is replaced by the larger Trp for JEV and DENV-2. This structural difference may explain why 4′-azido nucleoside analogs inhibit HCV but are inactive against JEV and DENV-2, as demonstrated in this study (compound 13) (29).

Because of its potency, compound 10 (DFMA) was chosen for *in vivo* studies using a model of DENV-2 infection in A129 mice. Treatment with compound 10 reduced DENV-2 loads in mice and ameliorated the disease pathology of infection. Compound 10 delivered as a preventative (day 0) or therapeutic (day 2 postinfection) modality prevented loss of body weight, mitigated viral induction of inflammation, and protected against hepatic edema. Hallmark features of human DHF/DSS are vascular leakage, greater viral burdens, elevated serum cytokine levels, hypotension, and thrombocytopenia (27, 28). Although leukopenia is a common feature found in patients with DENV infections, normal white blood cell counts or leukocytosis may also occur during DENV infections, as observed in experimental models (19, 20) and in children (30). Here we showed that compound 10 delivered as a preventative (day 0) or therapeutic (day 2 postinfection) modality prevented loss of body weight, mitigated viral induction of inflammation, ameliorated leukocytosis induced by infection, especially by reduction of circulating neutrophil levels, and protected against hepatic edema. Treatment with compound 10 reduced DENV-2 loads in several organs of mice, including the central nervous system (CNS), and ameliorated tissue damage due to infection. DENV is not classically considered a neurotropic virus, but it may cause encephalitis in humans (31, 32) and in immunosuppressed mice, including $A129^{-/-}$ and $AG129^{-/-}$ mice. Here we demonstrated that compound 10 was also able to prevent DENV dissemination to and replication in the CNS of A129 mice, suggesting that this compound may cross the blood-brain barrier.

Further investigation of the *in vivo* efficacy of compound 10 against JEV is recommended for future studies. These results support nucleoside analogs as attractive candidates for antiviral agents for DENV. Lee and colleagues (33) evaluated compound 5 in a different cell culture system and showed anti-DENV activity in Huh-7 cells but with an $EC_{50}$ of 11.2 $\mu$M for DENV-2, which was higher than our $EC_{50}$ value for DENV-2. They also showed *in vivo* antiviral activity of compound 5 when the compound was given immediately after virus inoculation but not when the compound was given in a therapeutic manner. In contrast, we observed that compound 10 was effective when given to A129 mice on a therapeutic schedule. It is unclear why a nucleoside analog was effective in our system but not in the study by Lee and colleagues (33). One possibility to explain such discrepancy is that we used A129 mice for our *in vivo* studies, whereas Lee and colleagues (33) used AG129 mice, which lack receptors for IFN-$\gamma$ in addition to lacking receptors for type I IFNs. In the context of DENV infection, several studies showed enhanced levels of IFN-$\gamma$ in DENV-infected humans, although the precise role of this cytokine in clinical DENV infections is somewhat controversial (34–36). Some studies suggested that levels of this cytokine may be positively correlated with disease in humans (36), but others showed that increased IFN-$\gamma$ production was correlated with higher survival rates in DHF patients (35). We showed previously that IFN-$\gamma$ plays an essential role in host resistance by controlling DENV replication through a mechanism dependent on nitric oxide production (19, 20). In the presence of IFN-$\gamma$, as in our A129 mice, compound 10 may interact positively with the host immune response to deal with the acute infection.

In conclusion, we identified two compounds with dual activity against JEV and all DENV serotypes at low micromolar concentrations. By inhibiting viral replication, these agents inhibit focus formation using infectious virus. The mouse experiments showed the potential of compound 10 for further studies, as it could decrease the viral loads in an infected animal model, with amelioration of the disease pathology. From molecular modeling studies of the DENV-2 and JEV RdRp replication complexes, we indirectly demonstrated that these compounds act on the conserved viral polymerase. These agents exhibited no significant toxicity in the cell lines used for the studies and serve as potential candidates for drug development. The approaches and findings presented here offer a rationale and promise to reduce the global burden of emerging or reemerging flaviviruses such as DENV and JEV.

## MATERIALS AND METHODS

**Cells and viruses.** C6/36 mosquito cells and African green monkey kidney (Vero) cells (ATCC) were grown and maintained in Eagle's minimum essential medium (EMEM) (Gibco) containing 10% fetal bovine serum (FBS) (Gibco), at 28°C and 37°C, respectively, in the presence of 5% $CO_2$. Baby hamster kidney (BHK-21) cell-derived replicon cell lines for DENV and JEV (BHK-DENV and BHK-JEV, respectively) (37) were grown in Dulbecco's minimum essential medium (DMEM) (Gibco) supplemented with 2% FBS and 1 mg/ml G418.

DENV-2 New Guinea C strain was used along with four distinct clinical DENV isolates, representative of the four DENV serotypes (DENV-1, DENV-2, DENV-3, and DENV-4). In addition, JEV Nakayama strain (GenBank accession number HE861351) was selected. For *in vivo* experiments, we used a clinical isolate of DENV-2 (strain 05K3295) from the Eden study in Singapore (38), which was kindly provided by Eng Ong Ooi from Duke-NUS Singapore. Viral stocks were propagated in C6/36 *Aedes albopictus* cells and titrated as described previously (19). Plaques were detected after 5 days of infection.

These viruses were identified and maintained at the virology laboratory of the Tropical Infectious Disease Research and Education Center, Faculty of Medicine, University of Malaya (Kuala Lumpur, Malaysia). C6/36 cells were infected with each DENV or JEV strain separately, and supernatants were harvested after observation of a cytopathic effect. Viral stocks were prepared and titrated on C6/36 cells using the focus-forming assay, as described previously, and were stored at −80°C for future experiments (39). Of note, during virus propagation and antiviral assays, the concentration of FBS was reduced to 2%.

**Nucleoside analogs.** Nucleoside derivatives (designated compounds 1 to 14) were synthesized in our laboratory according to previously reported procedures (29, 40–45) and were at least 95% pure, as estimated by liquid chromatography-mass spectrometry (LC-MS) and nuclear magnetic resonance (NMR) analyses. Chemical structures for compounds 1 to 14 are summarized in Fig. 1.

**Cytotoxicity assay.** The cytotoxicity of nucleoside analogs was evaluated *in vitro* using Vero and BHK-21 cells with an MTS assay kit (Promega, Madison, WI), according to the manufacturer's instructions. Briefly, monolayers of both cell lines were prepared in separate, 96-well, cell culture plates. The cells were treated with increasing concentrations of tested compounds in triplicate, followed by 4 days of incuba-

tion at 37°C. The MTS solution was then added, the cells were incubated for 4 h at 37°C, and resultant absorbance values for each well were determined at 570 nm using a 96-well plate reader (Tecan, Mannendorf, Switzerland). Concentration-response curves were constructed using GraphPad Prism 6 (GraphPad Software Inc., San Diego, CA, USA), and the $CC_{50}$ of each compound was calculated. Results were represented as the means ± standard deviations (SDs) from triplicate assays from three independent experiments.

**DENV and JEV replicon cellular assay systems.** The BHK-DENV and BHK-JEV replicon cell lines were plated at a density of $1 \times 10^4$ cells/well in separate, tissue culture-treated, white, 96-well plates (Promega). After 80% cell confluence was attained, the culture medium was replaced with DMEM containing 2% heat-inactivated FBS and different concentrations of tested compounds, in triplicate. Treated cells were then incubated for 48 h at 37°C with 5% $CO_2$. The culture medium was removed, and cells were lysed with 100 $\mu$l of lysis buffer (Promega) after washing with phosphate-buffered saline (PBS). The luciferase activity was evaluated according to the manufacturer's protocol (Promega). The luminescence signal was plotted against the logarithmically transformed concentrations of the tested compounds.

**Virus yield reduction assay.** Monolayers of Vero cells were prepared in 24-well cell culture microplates and overlaid for 1 h with DENV or JEV separately (multiplicity of infection of 0.1). After virus adsorption, cells were washed three times with cold sterile PBS to remove unattached viruses, and then the cells were treated for 2 days with increasing concentrations of the tested compounds. After 2 days, the supernatant was harvested and the yield of DENV or JEV was quantified using specific qRT-PCR for DENVs or JEV, respectively. The antiviral activity of each nucleoside analog was also investigated using a FFURA, as described previously (46, 47).

**DENV and JEV qRT-PCR.** DENV genomic RNA was extracted from the supernatants of infected cells on day 2 postinfection, using an RNA extraction kit (Qiagen, Hilden, Germany). Next, one-step qRT-PCR was carried out in a final volume of 20 $\mu$l containing 5 $\mu$l of diluted RNA, 1 $\mu$l of probe/primer mix, 10 $\mu$l of real-time master mix, and 4 $\mu$l of nuclease-free water (PrimerDesign, Southampton, UK). Quantitative PCR measurements were performed using a StepOnePlus real-time PCR system (Applied Biosystems, Foster City, CA, USA), according to the manufacturer's protocol. Raw data were analyzed with StepOne 2.2.1 software.

JEV extracellular genomic RNA (representative of JEV yield) was harvested from the JEV-infected Vero cells as described earlier. A JEV qRT-PCR assay was performed using the SensiMix SYBR green reagent (Quantace, Watford, UK) in a reaction mixture with JEV-specific forward and reverse primers (48, 49). All samples were assayed in triplicate. The amplifications were performed on the StepOnePlus real-time PCR system (Applied Biosystems), as described previously (47).

**Focus-forming unit reduction assay.** The antiviral activity of each compound was determined by measuring the reduction in the number of DENV or JEV infectious foci in Vero cells following treatment, as described previously (46, 47). Briefly, DENV- or JEV-infected Vero cells were treated at 48 h postinfection with increasing concentrations of each test compound and were incubated for 4 or 2 days (posttreatment), respectively. The antiviral activity of each compound was determined after visualizing and counting viral foci. Results were confirmed by the virus yield reduction assay using qRT-PCR.

**Molecular modeling of viral complexes.** The full-length JEV nonstructural protein 5 (NS5) (PDB accession no. 4K6M) and the DENV-2 NS5 (PDB accession no. 5K5M) were structurally aligned with the HCV RdRp replication complex with incoming ADP (PDB accession no. 4WTD) by using the MultiSeq tool in VMD (16–18, 50). This process identified sequences from parent DENV-2 and JEV crystals that were structurally analogous to those within 5.0 Å of the RNA template/primer and the active site in the HCV replication complex. Models of the NS5 RdRp replication complex were constructed using Prime chimeric homology modeling (Schrodinger Suite 2016-3; Schrödinger, LLC, New York, NY) with the OPLS3 force field. A model for the JEV replication complex (UniProtKB identifier P27395) used the HCV RdRp structural template for loops within 5 Å of nucleic acids and the full-length JEV template of PDB accession no. 4K6M for non-active-site sequences. The model was built using the knowledge-based approach in the module and included the RNA template/primer, active site ATP from the cocrystallized ADP, and active site $Mn^{2+}$ ions from the HCV crystal. The priming loop (residues 789 to 808) was deleted because of artifactual positioning that clashed with the RNA template/primer. The active site was visually inspected to correct poor residue positioning (e.g., Trp536), and the structure was minimized using Prime gradient minimization with the OPLS3 force field. A final minimization was performed with Prime molecular mechanics-generalized Born and surface area (MM-GBSA) scoring, with the ligand of interest bound to the active site and optimization of residues within 5.0 Å. A model of the DENV-2 RdRp replication complex was constructed using the same work flow with the template structure of PDB accession no. 5K5M. This structure was selected for DENV because it provided the best positioning of an active site loop (residues 455 to 472) that was absent in other reported structures.

**Ethics statement for mouse studies.** The study was performed in strict accordance with the ethical and animal experiment regulations of the Brazilian government (law 11794/2008). The experimental protocol was approved by the Committee on Animal Ethics of the Universidade Federal de Minas Gerais (permit protocol 169/2016). All surgery was performed under ketamine/xylazine anesthesia, and all efforts were made to minimize animal suffering. Studies with DENV-2 were conducted under biosafety level 2 containment at the immunopharmacology laboratory of the Instituto de Ciencias Biológicas at the Universidade Federal de Minas Gerais, Brazil.

For *in vivo* experiments, A129 mice (deficient for the type I IFN receptor [IFN$\alpha/\beta R^{-/-}$] and originally from The Jackson Laboratory [reference no. 010830]) were obtained from Bioterio de Matrizes da Universidade de Sao Paulo. Adult mice (7 to 9 weeks of age) were kept under specific-pathogen-free conditions. A159 mice (5 to 8 mice per group) were inoculated with $1 \times 10^3$ PFU DENV-2 (strain 05K3295)

by the i.p. route. Disease signs (presence of ruffled fur, partial or complete hindlimb weakness or paralysis, and loss of body weight) were monitored daily. Moribund mice with ≥10% body weight loss were euthanized; this time point generally occurred between day 3 and day 6 after DENV-2 inoculation (peak of DENV infection). In parallel, some mice received pretreatment (from day 0 to day 6) or therapeutic treatment (from day 2 to day 6) once a day, via the i.p. route, with compound 10 diluted in 200 μl of PBS, at a dose of 10 mg/kg per day. Vehicle-treated mice received 200 μl of PBS once a day, via the i.p. route.

**Titration of virus.** Viral loads in serum and mouse tissues (spleen, liver, and brain) were assessed by a plaque assay in Vero cells, as described previously (51). Results were measured as PFU per gram of tissue weight or milliliter of supernatant.

**Hematological analysis.** Blood was obtained from the vena cava, in heparin-containing syringes, on day 6 of DENV-2 infection. Platelets were analyzed as described (51). Total leukocyte counts were obtained by using a Neubauer chamber. Differential counts were determined with staining with a Panotico kit (Interlab) and subsequently were quantified microscopically in blood smears from each mouse.

**MPO activity assay.** The extent of neutrophil accumulation in the spleen and brain of control and DENV-infected mice was measured by assaying MPO activity, as described previously (19).

**Measurement of cytokine and chemokine concentrations.** The concentrations of the cytokine (IL-6) and the chemokine (CCL5) in the serum of control and DENV-infected mice were measured using commercially available antibodies, according to the procedures supplied by the manufacturer (R&D Systems).

**Histopathological analysis.** Liver samples from euthanized mice were obtained on day 6 after DENV-2 infection. Histopathological analyses were performed as described (19). Briefly, after collection, samples were immediately fixed in 10% buffered formalin for 48 h and embedded in paraffin. Tissue sections (thickness, 4 μm) were stained with hematoxylin and eosin and evaluated under a microscope (Axioskop 40; Carl Zeiss, Göttingen, Germany) adapted to a digital camera (PowerShot A620; Canon, Tokyo, Japan). Histopathology scoring was performed as adapted from reference 19, evaluating hepatocyte swelling and degeneration and cellular infiltration/hemorrhage, on a 4-point scale (0, absent; 1, minimal; 2, moderate; 3, serious; 4, severe), in each analysis. For easy interpretation, the overall score was taken into account, and all of the parameters totaled 12 points. A total of two sections for each animal were examined, and the results were plotted as the median of damage values for each mouse.

**Statistical analysis.** The $EC_{50}$ and $CC_{50}$ values for the tested compounds were determined using GraphPad Prism for Windows 5 (Graph Pad Software), as the means ± standard errors of the mean (SEMs) from triplicate assays from three independent experiments. Selectivity index values were calculated as the $CC_{50}/EC_{50}$ ratio for each compound. For *in vivo* experiments, results are shown as means ± SDs except for viral loads, which were expressed as medians. Body weight loss was calculated by subtracting the baseline values obtained before infection. Differences were compared by using analysis of variance, followed by Student-Newman-Keuls *post hoc* analysis or, alternatively, *t* tests using nonparametric analysis (Mann-Whitney test). GraphPad Prism 5.0 software was used for all analyses. Results with *P* values of $<0.05$ were considered significant.

## ACKNOWLEDGMENTS

This work was supported in part by the NIH (grant R21-AI-129607) and by the Emory University Center for AIDS Research (NIH grant 2P30-AI-050409 to R.F.S.). This study was also supported by the Ministry of Higher Education, Malaysia (high-impact research grant E000087-20001 and long-range scheme grant LR001/2011F). This work received financial support from the National Institute of Science and Technology in Dengue and Host-Microorganism Interaction, a program funded by the Brazilian National Science Council (Brazil), the Minas Gerais Foundation for Science (Brazil), and the Comissao de Apoio a Pessoal de Ensino Superior (Brazil).

We declare no conflicts of interest.

## REFERENCES

1. Messina JP, Brady OJ, Scott TW, Zou C, Pigott DM, Duda KA, Bhatt S, Katzelnick L, Howes RE, Battle KE, Simmons CP, Hay SI. 2014. Global spread of dengue virus types: mapping the 70 year history. Trends Microbiol 22:138–146. https://doi.org/10.1016/j.tim.2013.12.011.
2. Gubler DJ, Ooi EE, Vasudevan S, Farrar J (eds). 2014. Dengue and dengue hemorrhagic fever, 2nd ed. CABI, Wallingford, UK.
3. Guzman MG, Halstead SB, Artsob H, Buchy P, Farrar J, Gubler DJ, Hunsperger E, Kroeger A, Margolis HS, Martínez E, Nathan MB, Pelegrino JL, Simmons C, Yoksan S, Peeling RW. 2010. Dengue: a continuing global threat. Nat Rev Microbiol 8:S7–S16. https://doi.org/10.1038/nrmicro2460.
4. Wang H, Liang G. 2015. Epidemiology of Japanese encephalitis: past, present, and future prospects. Ther Clin Risk Manag 11:435. https://doi.org/10.2147/TCRM.S51168.
5. Paul W, Moore P, Karabatsos N, Flood S, Yamada S, Jackson T, Tsai T. 1993. Outbreak of Japanese encephalitis on the island of Saipan, 1990. J Infect Dis 167:1053–1058. https://doi.org/10.1093/infdis/167.5.1053.
6. Wakai S. 1998. Scourge of Japanese encephalitis in south-western Nepal. Lancet 351:759. https://doi.org/10.1016/S0140-6736(05)78540-8.
7. Unni SK, Růžek D, Chhatbar C, Mishra R, Johri MK, Singh SK. 2011. Japanese encephalitis virus: from genome to infectome. Microbes Infect 13:312–321. https://doi.org/10.1016/j.micinf.2011.01.002.
8. Solomon T, Dung NM, Kneen R, Gainsborough M, Vaughn DW, Khanh VT. 2000. Japanese encephalitis. J Neurol Neurosurg Psychiatry 68:405–415. https://doi.org/10.1136/jnnp.68.4.405.
9. Hennessy S, Strom BL, Bilker WB, Zhengle L, Chao-Min W, Hui-Lian L, Tai-Xiang W, Hong-Ji Y, Qi-Mau L, Tsai TF, Karabatsos N, Strom BL,

Halstead SB. 1996. Effectiveness of live-attenuated Japanese encephalitis vaccine (SA14-14-2): a case-control study. Lancet 347:1583–1586. https://doi.org/10.1016/S0140-6736(96)91075-2.
10. Dans AL, Dans LF, Lansang MAD, Silvestre MAA, Guyatt GH. 2018. Review of a licensed dengue vaccine: inappropriate subgroup analyses and selective reporting may cause harm in mass vaccination programs. J Clin Epidemiol 95:137–139. https://doi.org/10.1016/j.jclinepi.2017.11.019.
11. Grady D, Thomas K. 17 December 2017. Drug company under fire after revealing dengue vaccine may harm some. New York Times, New York, NY https://www.nytimes.com/2017/12/17/health/sanofi-dengue-vaccine-philippines.html.
12. Bhatia HK, Singh H, Grewal N, Natt NK. 2014. Sofosbuvir: a novel treatment option for chronic hepatitis C infection. J Pharmacol Pharmacother 5:278. https://doi.org/10.4103/0976-500X.142464.
13. Schinazi RF. 2003. Emtricitabine: a viewpoint. Drugs 63:2425–2426. https://doi.org/10.2165/00003495-200363220-00004.
14. Rawlinson SM, Pryor MJ, Wright PJ, Jans DA. 2006. Dengue virus RNA polymerase NS5: a potential therapeutic target? Curr Drug Targets 7:1623–1638. https://doi.org/10.2174/138945006779025383.
15. Lim SP, Noble CG, Shi P-Y. 2015. The dengue virus NS5 protein as a target for drug discovery. Antiviral Res 119:57–67. https://doi.org/10.1016/j.antiviral.2015.04.010.
16. Appleby TC, Perry JK, Murakami E, Barauskas O, Feng J, Cho A, Fox D, Wetmore DR, McGrath ME, Ray AS, Sofia MJ, Swaminathan S, Edwards TE. 2015. Structural basis for RNA replication by the hepatitis C virus polymerase. Science 347:771–775. https://doi.org/10.1126/science.1259210.
17. Lu G, Gong P. 2013. Crystal structure of the full-length Japanese encephalitis virus NS5 reveals a conserved methyltransferase-polymerase interface. PLoS Pathog 9:e1003549. https://doi.org/10.1371/journal.ppat.1003549.
18. Lim SP, Noble CG, Seh CC, Soh TS, El Sahili A, Chan GKY, Lescar J, Arora R, Benson T, Nilar S, Manjunatha U, Wan KF, Dong H, Xie X, Shi P-Y, Yokokawa F. 2016. Potent allosteric dengue virus NS5 polymerase inhibitors: mechanism of action and resistance profiling. PLoS Pathog 12:e1005737. https://doi.org/10.1371/journal.ppat.1005737.
19. Costa VV, Fagundes CT, Valadão DF, Cisalpino D, Dias ACF, Silveira KD, Kangussu LM, Ávila TV, Bonfim MRQ, Bonaventura D, Silva TA, Sousa LP, Rachid MA, Vieira LQ, Menezes GB, de Paula AM, Atrasheuskaya A, Ignatyev G, Teixeira MM, Souza DG. 2012. A model of DENV-3 infection that recapitulates severe disease and highlights the importance of IFN-γ in host resistance to infection. PLoS Negl Trop Dis 6:e1663. https://doi.org/10.1371/journal.pntd.0001663.
20. Fagundes CT, Costa VV, Cisalpino D, Amaral FA, Souza PRS, Souza RS, Ryffel B, Vieira LQ, Silva TA, Atrasheuskaya A, Ignatyev G, Sousa LP, Souza DG, Teixeira MM. 2011. IFN-γ production depends on IL-12 and IL-18 combined action and mediates host resistance to dengue virus infection in a nitric oxide-dependent manner. PLoS Negl Trop Dis 5:e1449. https://doi.org/10.1371/journal.pntd.0001449.
21. Ojha A, Nandi D, Batra H, Singhal R, Annarapu GK, Bhattacharyya S, Seth T, Dar L, Medigeshi GR, Vrati S, Vikram NK, Guchhait P. 2017. Platelet activation determines the severity of thrombocytopenia in dengue infection. Sci Rep 7:41697. https://doi.org/10.1038/srep41697.
22. Schexneider K, Reedy E. 2005. Thrombocytopenia in dengue fever. Curr Hematol Rep 4:145–148.
23. Costa VV, Ye W, Chen Q, Teixeira MM, Preiser P, Ooi EE, Chen J. 2017. Dengue virus-infected dendritic cells, but not monocytes, activate natural killer cells through a contact-dependent mechanism involving adhesion molecules. mBio 8:e00741-17. https://doi.org/10.1128/mBio.00741-17.
24. Kohler JJ, Nettles JH, Amblard F, Hurwitz SJ, Bassit L, Stanton RA, Ehteshami M, Schinazi RF. 2014. Approaches to hepatitis C treatment and cure using NS5A inhibitors. Infect Drug Resist 7:41. https://doi.org/10.2147/IDR.S36247.
25. Carroll SS, Olsen D. 2006. Nucleoside analog inhibitors of hepatitis C virus replication. Infect Disord Drug Targets 6:17–29. https://doi.org/10.2174/187152606776056698.
26. Cox BD, Stanton RA, Schinazi RF. 2015. Predicting Zika virus structural biology: challenges and opportunities for intervention. Antivir Chem Chemother 24:118–126. https://doi.org/10.1177/2040206616653873.
27. Halstead SB. 2007. Dengue. Lancet 370:1644–1652. https://doi.org/10.1016/S0140-6736(07)61687-0.
28. Balmaseda A, Hammond SN, Pérez L, Tellez Y, Saborío SI, Mercado JC, Cuadra R, Rocha J, Pérez MA, Silva S, Rocha C, Harris E. 2006. Serotype-specific differences in clinical manifestations of dengue. Am J Trop Med Hyg 74:449–456. https://doi.org/10.4269/ajtmh.2006.74.449.
29. Rondla R, Coats SJ, McBrayer TR, Grier J, Johns M, Tharnish PM, Whitaker T, Zhou L, Schinazi RF. 2009. Anti-hepatitis C virus activity of novel β-D-2′-*C*-methyl-4′-azido pyrimidine nucleoside phosphoramidate prodrugs. Antivir Chem Chemother 20:99–106. https://doi.org/10.3851/IMP1400.
30. Khandelwal RK. 2017. Effect of dengue fever on the total leucocyte count and neutrophil count in children in early febrile period. Int J Pediatr Res 4:617–622.
31. Madi D, Achappa B, Ramapuram JT, Chowta N, Laxman M, Mahalingam S. 2014. Dengue encephalitis: a rare manifestation of dengue fever. Asian Pac J Trop Biomed 4(Suppl):S70–S72. https://doi.org/10.12980/APJTB.4.2014C1006.
32. Baldaçara L, Ferreira JR, Filho LCPS, Venturini RR, Coutinho OMVC, Camarço WC, Fernandes CC, Júnior EV. 2013. Behavior disorder after encephalitis caused by dengue. J Neuropsychiatry Clin Neurosci 25:E44. https://doi.org/10.1176/appi.neuropsych.12020040.
33. Lee J-C, Tseng C-K, Wu Y-H, Kaushik-Basu N, Lin C-K, Chen W-C, Wu H-N. 2015. Characterization of the activity of 2′-*C*-methylcytidine against dengue virus replication. Antiviral Res 116:1–9. https://doi.org/10.1016/j.antiviral.2015.01.002.
34. Chen R-F, Liu J-W, Yeh W-T, Wang L, Chang J-C, Yu H-R, Cheng J-T, Yang KD. 2005. Altered T helper 1 reaction but not increase of virus load in patients with dengue hemorrhagic fever. FEMS Immunol Med Microbiol 44:43–50. https://doi.org/10.1016/j.femsim.2004.11.012.
35. Chen L-C, Lei H-Y, Liu C-C, Shiesh S-C, Chen S-H, Liu H-S, Lin Y-S, Wang S-T, Shyu H-W, Yeh T-M. 2006. Correlation of serum levels of macrophage migration inhibitory factor with disease severity and clinical outcome in dengue patients. Am J Trop Med Hyg 74:142–147. https://doi.org/10.4269/ajtmh.2006.74.142.
36. Bozza FA, Cruz OG, Zagne SM, Azeredo EL, Nogueira RM, Assis EF, Bozza PT, Kubelka CF. 2008. Multiplex cytokine profile from dengue patients: MIP-1beta and IFN-gamma as predictive factors for severity. BMC Infect Dis 8:86. https://doi.org/10.1186/1471-2334-8-86.
37. Yang C-C, Tsai M-H, Hu H-S, Pu S-Y, Wu R-H, Wu S-H, Lin H-M, Song J-S, Chao Y-S, Yueh A. 2013. Characterization of an efficient dengue virus replicon for development of assays of discovery of small molecules against dengue virus. Antiviral Res 98:228–241. https://doi.org/10.1016/j.antiviral.2013.03.001.
38. Low JG, Ooi E, Tolfvenstam T, Leo Y-S, Hibberd ML, Ng L-C, Lai Y-L, Yap G, Li C, Vasudevan SG. 2006. Early dengue infection and outcome study (EDEN): study design and preliminary findings. Ann Acad Med Singapore 35:783–789.
39. Zandi K, Teoh B-T, Sam S-S, Wong P-F, Mustafa MR, AbuBakar S. 2012. Novel antiviral activity of baicalein against dengue virus. BMC Complement Altern Med 12:214. https://doi.org/10.1186/1472-6882-12-214.
40. Zhou L, Zhang H, Tao S, Ehteshami M, Cho JH, McBrayer TR, Tharnish P, Whitaker T, Amblard F, Coats SJ, Schinazi RF. 2016. Synthesis and evaluation of 2,6-modified purine 2′-*C*-methyl ribonucleosides as inhibitors of HCV replication. ACS Med Chem Lett 7:17–22. https://doi.org/10.1021/acsmedchemlett.5b00402.
41. Eldrup AB, Prhavc M, Brooks J, Bhat B, Prakash TP, Song Q, Bera S, Bhat N, Dande P, Cook PD, Bennett CF, Carroll SS, Ball RG, Bosserman M, Burlein C, Colwell LF, Fay JF, Flores OA, Getty K, LaFemina RL, Leone J, MacCoss M, McMasters DR, Tomassini JE, Von Langen D, Wolanski B, Olsen DB. 2004. Structure-activity relationship of heterobase-modified 2′-*C*-methyl ribonucleosides as inhibitors of hepatitis C virus RNA replication. J Med Chem 47:5284–5297. https://doi.org/10.1021/jm040068f.
42. Sari O, Bassit L, Gavegnano C, McBrayer TR, McCormick L, Cox B, Coats SJ, Amblard F, Schinazi RF. 2017. Synthesis and antiviral evaluation of 2′,2′,3′,3′-tetrafluoro nucleoside analogs. Tetrahedron Lett 58:642–644. https://doi.org/10.1016/j.tetlet.2017.01.006.
43. Hatton W, Hunault J, Egorov M, Len C, Pipelier M, Blot V, Silvestre V, Fargeas V, Ané A, McBrayer T, Detorio M, Cho J-H, Bourgougnon N, Dubreuil D, Schinazi RF, Lebreton J. 2011. Synthesis and biological evaluation of 4′–C,3′–*O*-propylene-linked bicyclic nucleosides. Eur J Org Chem 2011:7390–7399. https://doi.org/10.1002/ejoc.201100859.
44. Smith DB, Kalayanov G, Sund C, Winqvist A, Maltseva T, Leveque VJ-P, Rajyaguru S, Pogam SL, Najera I, Benkestock K, Zhou X-X, Kaiser AC, Maag H, Cammack N, Martin JA, Swallow S, Johansson NG, Klumpp K, Smith M. 2009. The design, synthesis, and antiviral activity of monofluoro and difluoro analogues of 4′-azidocytidine against hepatitis C virus replication: the discovery of 4′-azido-2′-deoxy-2′-fluorocytidine

and 4′-azido-2′-dideoxy-2′, 2′-difluorocytidine. J Med Chem 52:2971–2978. https://doi.org/10.1021/jm801595c.
45. Sofia MJ, Bao D, Chang W, Du J, Nagarathnam D, Rachakonda S, Reddy PG, Ross BS, Wang P, Zhang H-R, Bansal S, Espiritu C, Keilman M, Lam AM, Steuer HMM, Niu C, Otto MJ, Furman PA. 2010. Discovery of a β-D-2′-deoxy-2′-α-fluoro-2′-β-C-methyluridine nucleotide prodrug (PSI-7977) for the treatment of hepatitis C virus. J Med Chem 53:7202–7218. https://doi.org/10.1021/jm100863x.
46. Moghaddam E, Teoh B-T, Sam S-S, Lani R, Hassandarvish P, Chik Z, Yueh A, Abubakar S, Zandi K. 2014. Baicalin, a metabolite of baicalein with antiviral activity against dengue virus. Sci Rep 4:5452.
47. Johari J, Kianmehr A, Mustafa MR, Abubakar S, Zandi K. 2012. Antiviral activity of baicalein and quercetin against the Japanese encephalitis virus. Int J Mol Sci 13:16785–16795. https://doi.org/10.3390/ijms131216785.
48. Santhosh SR, Parida MM, Dash PK, Pateriya A, Pattnaik B, Pradhan HK, Tripathi NK, Ambuj S, Gupta N, Saxena P, Lakshmana Rao PV. 2007. Development and evaluation of SYBR Green I-based one-step real-time RT-PCR assay for detection and quantification of chikungunya virus. J Clin Virol 39:188–193. https://doi.org/10.1016/j.jcv.2007.04.015.
49. Park S-I, Park D-H, Saif LJ, Jeong Y-J, Shin D-J, Chun Y-H, Park S-J, Kim H-J, Hosmillo M, Kwon H-J, Kang M-I, Cho K-O. 2009. Development of SYBR Green real-time RT-PCR for rapid detection, quantitation and diagnosis of unclassified bovine enteric calicivirus. J Virol Methods 159:64–68. https://doi.org/10.1016/j.jviromet.2009.03.001.
50. Humphrey W, Dalke A, Schulten K. 1996. VMD: visual molecular dynamics. J Mol Graph 14:33–38. https://doi.org/10.1016/0263-7855(96)00018-5.
51. Costa VV, Fagundes CT, Valadão DF, Ávila TV, Cisalpino D, Rocha RF, Ribeiro LS, Ascenção FR, Kangussu LM, Junior CMQ, Astigarraga RG, Gouveia FL, Silva TA, Bonaventura D, de Almeida Sampaio D, Leite ACL, Teixeira MM, Souza DG. 2014. Subversion of early innate antiviral responses during antibody-dependent enhancement of dengue virus infection induces severe disease in immunocompetent mice. Med Microbiol Immunol 203:231–250. https://doi.org/10.1007/s00430-014-0334-5.